Australian Government
Department of Agriculture, Fisheries and Forestry

Technical Report

Program and KPI: Sub-program 1.2 KPI 3.11

Report Title: DEXA Accreditation algorithm update

Prepared by: Dr Steve Connaughton and Professor Graham Gardner
Murdoch University

Date published: 30 January 2023

This project is supported by funding from the Australian Government Department of Agriculture, Fisheries and Forestry as part of its Rural R&D for Profit programme in partnership with Research & Development Corporations, Commercial Companies, State Departments & Universities.

Abstract

An accredited algorithm for the prediction of lamb carcass composition was submitted and accepted by AUSMEAT in September 2022, a report of which can be found as technical report 3.11 – Lamb DXA accreditation submission to AMILSC on behalf of Scott Automation and Robotics and MLA. That technical report shows the results of the algorithm's predictions, and what bands of weight and composition the algorithm is accredited for.

This technical report details the algorithm that was used, and the method of training and calibration using the Scott Automation and Robotics phantom.

This project is supported by funding from the Australian Government Department of Agriculture, Fisheries and Forestry as part of its Rural R&D for Profit programme in partnership with Research & Development Corporations, Commercial Companies, State Departments & Universities.

Contents

This project is supported by funding from the Australian Government Department of Agriculture, Fisheries and Forestry as part of its Rural R&D for Profit programme in partnership with Research & Development Corporations, Commercial Companies, State Departments & Universities.

1 Introduction

Ongoing improvements with the algorithm that drives the DXA predictions of CT carcass composition have resulted in an overall algorithm that has achieved accreditation with AUSMEAT, the report of which can be found in 3.11 - Lamb DXA accreditation submission to AMILSC on behalf of Scott Automation and Robotics and MLA. There are two large improvements that have been made with the accredited algorithm from its predecessor: the ability to detect bone has been reworked and improved (3.11.5.b) and the daily calibration-adjustments that are made using information drawn from the start-of-day scan of the Scott Automation and Robotics phantom. The equation for detecting fat and fat free mass of soft tissue through a function of the R-value and thickness of the tissue, using unique coefficients for each system by the following equation:

$$Fat\ \% = a + bR + ct + dRT + eR^2 + ft^2 \qquad Eq.1$$

Where a-f are the unique coefficients, R is R-value, and t is thickness, or a proxy thereof from the logarithm of the low or high energy value. The previous algorithm used a form of this equation to determine an overall soft tissue DXA value, which was linearly transformed to calculate the prediction of fat % and lean %. Despite the bone containing pixels being excluded from the calculation of the DXA value, it was still used in its own linear transformation to predict bone %. While there was some accuracy and precision with the prediction of CT determined bone %, using the soft tissue values to predict bone resulted in prediction of this tissue type being the least precise.

2 Accredited Algorithm

2.1 Daily Calibration

2.1.1 Process

Each day, prior to the start of production, a synthetic phantom constructed of nylon, polyethylene, and acrylic (Figure 1) is scanned, referred to as the phantom image, along with the unattenuated space with and without the production of x-rays, referred to as the light and dark calibration images. These images are saved each day and can be accessed along with the lamb images produced during the day.

There are varying mixtures and depths of these three plastics, resulting in up to 40 plastic combinations that can be scanned in a single image. Due to detector orientation, it is not always possible to image all 40 combinations, as some are cut from the top of bottom of the image, however the entirety of the detector height can be covered. This enables multiple sampling of the same plastic at different heights.

This project is supported by funding from the Australian Government Department of Agriculture, Fisheries and Forestry as part of its Rural R&D for Profit programme in partnership with Research & Development Corporations, Commercial Companies, State Departments & Universities.

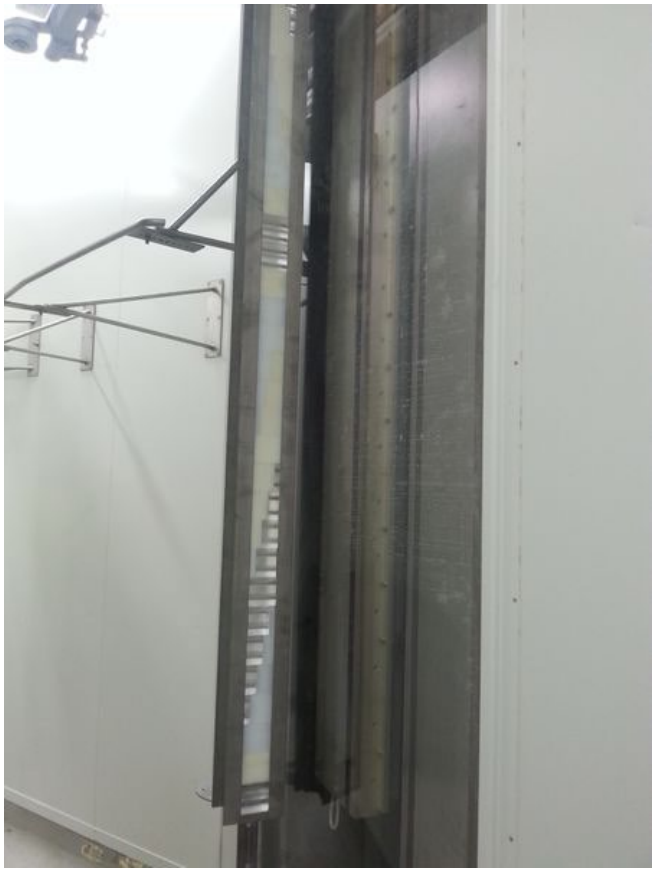

Figure 1 - Scott Automation and Robotics synthetic phantom block

Each portion of the plastic phantom has a linear attenuation coefficient unique to the material at a given energy. The attenuation can be mapped and visualised in Figure 2, which is a calibration scan taken at the start of days processing at the WAMMCO facility.

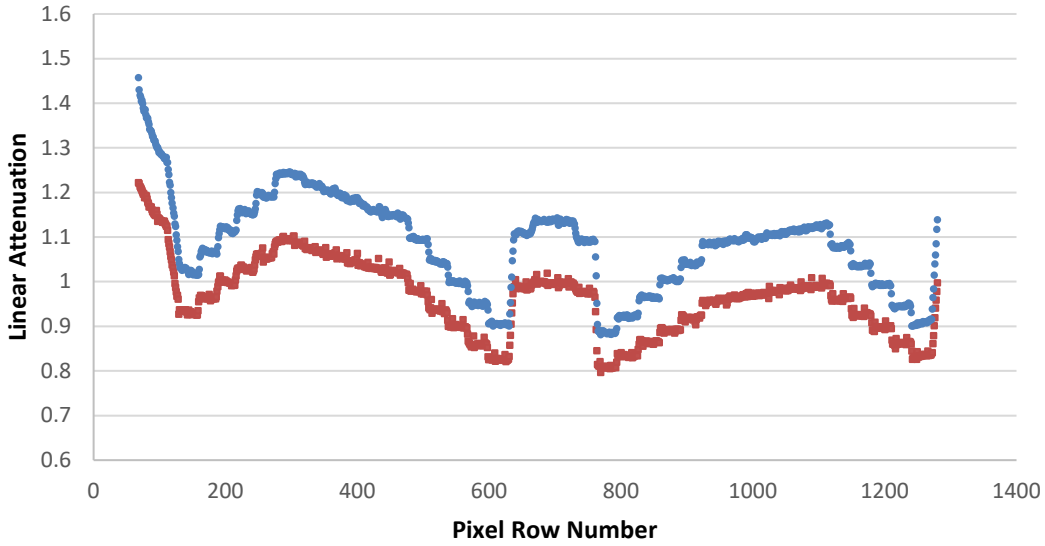

Figure 2 - Attenuation for each pixel row for the WAMMCO start of day calibration, red points represent high energy image, blue represents low energy image

This project is supported by funding from the Australian Government Department of Agriculture, Fisheries and Forestry as part of its Rural R&D for Profit programme in partnership with Research & Development Corporations, Commercial Companies, State Departments & Universities.

2.1.2 Coefficient Calculation

From these calibration scans, it is possible to make changes to the coefficients found in Equation 1 to maintain accuracy of the DXA predictions. The R-value and thickness coefficients can be changed for the soft tissue calculations, as well as any coefficients for weight predictions and bone predictions. The specific adjustments that would be made are found in the following sections.

2.2 Image Standardisation

This portion of the algorithm has not been amended from its original version, and is designed to account for R-value drift through each days production. In summary, each pixel of the image being standardised is compared to the start of day light and dark images to calibrate their unattenuated value to 4095. This is achieved by the following equation:

$$CalibratedPixel[x,y] = 4095 * \frac{RawPixel[x,y] - DarkImage[y]}{LightImage[y] - DarkImage[y]} \qquad Eq.2$$

The unattenuated space around each carcass is then continuously sampled throughout the day, and if the row mean differs from 4095, the whole row is adjusted by this difference. This ensures a consistent attenuation ratio for calculation in future steps. This process is repeated for both the high and low energy images to create two standardised images.

2.3 Removal of non-carcass containing pixels

The next processing step involves the removal of “non-carcase” unattenuated pixels by eliminating those with values that exceed the threshold value of 3700. This step is applied to both the high and low energy images.

2.4 R-value calculation

The R-value for each pixel is calculated by the following equation:

$$R = \frac{\ln\left(\frac{PixelLow[x,y]}{4095}\right)}{\ln\left(\frac{PixelHigh[x,y]}{4095}\right)} \qquad Eq.3$$

The value of each pixel is then “smoothed” by a convolution kernel, weighting each of its neighbouring pixels with itself by the kernel expressed below:

0.093198052	0.131801948	0.093198052
0.131801948	0.1	0.131801948
0.093198052	0.131801948	0.093198052

This project is supported by funding from the Australian Government Department of Agriculture, Fisheries and Forestry as part of its Rural R&D for Profit programme in partnership with Research & Development Corporations, Commercial Companies, State Departments & Universities.

Where each of the values represent the proportion of that pixels value on the final value of the smoothed pixel in the centre of the 3x3 grid.

R-values that are above 2 or below 1 are deemed errors and are removed from any further calculations. Furthermore, any low energy pixels with a value less than 50 is removed from further calculations, as this represents a thickness of tissue that has been shown to yield unreliable R-values.

2.5 Bone Detection

Bone detection is achieved by the technique described in 3.11.5b.

Briefly, a proxy value for the thickness of each pixel is determined by the equation:

$$thickness = \ln(I_L) \qquad Eq.4$$

The R-value of each pixel is then squared and then divided by the proxy thickness value and processed as a natural logarithm, as per the following equation:

$$\ln\left(\frac{R^2}{thickness}\right) \qquad Eq.5$$

This final value is evaluated relative to a threshold, with pixels exceeding this threshold deemed to contain bone, The value threshold is yet to be automatically generated by the accreditation algorithm, as there has not been enough points of data from enough different DXA units with phantom calibration capabilities to train this. However, thresholds for WAMMCO and GMP have been manually calculated, and do not change from day-to-day calibration readings. This will become automated in future iterations of the algorithm.

2.6 Bone Content Calculation

2.6.1 Equation

The ratio of bone containing pixels to total pixels is calculated from the bone detection step and given the term *BST*. The mean R-value of the bone containing pixels is also calculated, and given the term *BR*. The R-values of the bone containing pixels may vary between different DXA machines, and the coefficient is adjusted accordingly and given the value *BRΔ*, which is further described below. The percentage of bone in the carcass is then calculated by the equation:

$$Bone\ \% = -104.34 + 21.76 * BST + BR\Delta * BR \qquad Eq.6$$

2.6.2 Training Set

This was trained on 620 carcasses that were also CT scanned for bone %. The prediction of DXA bone % is a regressed general linear model, which included all outputted variables from the carcass and their interactions.

This project is supported by funding from the Australian Government Department of Agriculture, Fisheries and Forestry as part of its Rural R&D for Profit programme in partnership with Research & Development Corporations, Commercial Companies, State Departments & Universities.

2.6.3 Calibration variable

The variable *BRΔ* is calculated through use of the Scott phantom, reading only the acrylic portions of the phantom, and using the mean R-values according to their linear attenuation coefficients. This enables the R-value to be independent of thickness in this calculation. The coefficient is adjusted by the following equation:

$$BR\Delta = -613.23 * AcrylicR + 800.82 \qquad Eq.7$$

2.7 Soft Tissue Evaluation

2.7.1 Weight calculation

The weight of soft tissue in the carcass is heavily related to HCWT, however a prediction of the soft tissue weight can be improved upon by the inclusion of *BST* and the thickness proxy described in Equation 4, which will be termed *t* for the soft tissue thickness proxy. The coefficient for *t (tΔ)* can be adjusted based on the Scott phantom calibration, with the equation discussed below. The soft tissue weight prediction equation is:

$$STWt = -4.0348 * BST + 0.8452 * HCWT + 11.1872 - 1.54563 * t\Delta * t \qquad Eq.8$$

This produced highly precise and accurate predictions of soft tissue weight, as seen in Figure 3. This can also be used as a check for the bone % prediction, as they are calculating the same value using different vectors.

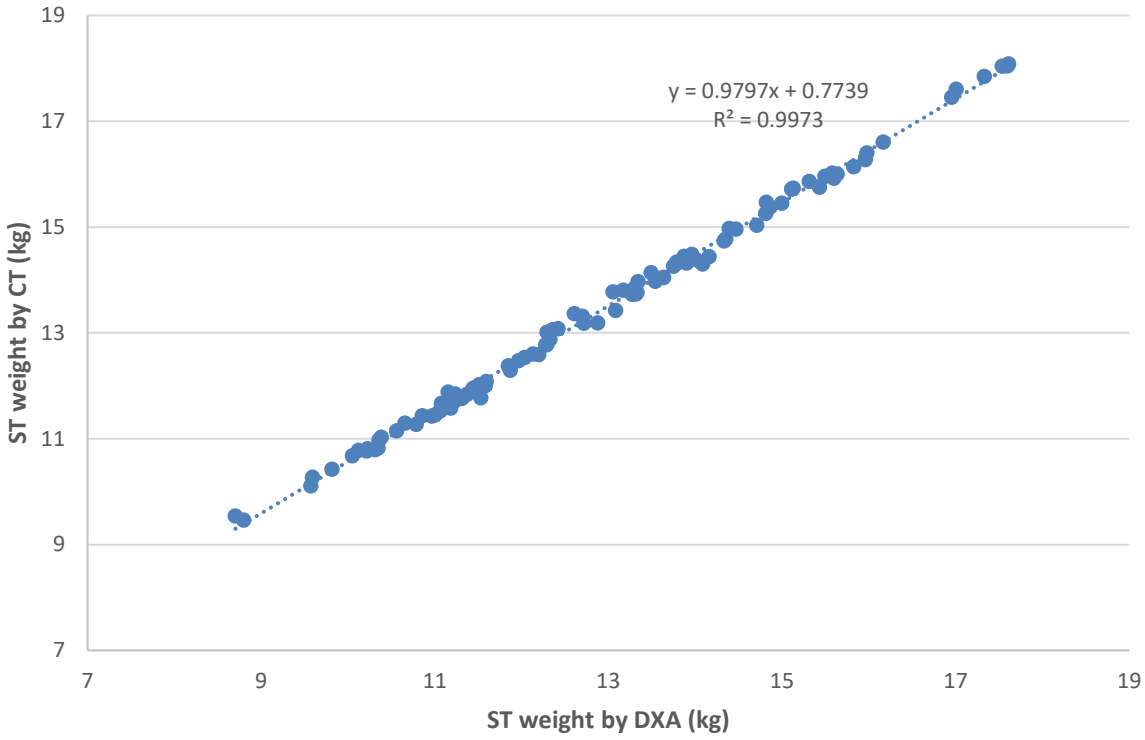

Figure 3 - Prediction of soft tissue (ST) weight by DXA compared to CT in 100 lambs. DXA unit was located in WAMMCO, Katanning.

This project is supported by funding from the Australian Government Department of Agriculture, Fisheries and Forestry as part of its Rural R&D for Profit programme in partnership with Research & Development Corporations, Commercial Companies, State Departments & Universities.

2.7.2 Fat proportion in soft tissue calculation

The fat proportion in soft tissue is calculated by a variation of Equation 1, with some coefficients adjusted by the Scott phantom. The mean R-value of all soft tissue pixels, and the mean of the thickness proxy is calculated for use in the equation. The R-values and thickness proxies can be adjusted by the Scott phantom, with all other coefficients remaining the same, as per the equation:

$$FatLean\% = -8558.84 - 1982.08t - 25572R - 16724R^2 + 2170.54Rt - 48.5423t^2 \quad Eq.9$$

Where *FatLean%* is the proportion of fat in the soft tissue, *t* is the thickness proxy for soft tissue pixels, and *R* is the mean R-value of the soft tissue pixels

2.7.3 Training

The soft tissue weight and fat to lean ratio equations were trained on 620 lamb carcasses, with CT composition as the predicted value. In the case of soft tissue weight, the value being predicted was the soft tissue component of the carcass as determined by CT scanning, multiplied by the HCWT as per the equation:

$$STwt[CT] = \frac{CT\ fat\ \% + CT\ Lean\ \%}{100} * HCWT \qquad Eq.10$$

The proportion of fat in soft tissue was set as the proportion of CT fat % within the total soft tissue component determined by CT, as per the equation:

$$FatLean\%[CT] = \frac{(CT\ fat\ \%)}{CT\ fat\ \% + CT\ lean\ \%} * 100 \qquad Eq.11$$

The accredited equation is a general linear model with the fundamental variables included as per Equation 1.

2.7.4 Calibration variable

The R-value for soft tissue (*STR*) and the thickness proxy (*t*) can be adjusted using the Scott phantom. *t* change (*tΔ*) is calculated through the division of the *STLE* of acrylic within the Scott phantom by a set value of 7.184091653, as determined by initial calibration and standardisation of the WAMMCO site. The *tΔ* for GMP, for example, is 0.956.

The *STR* value change (*STRΔ*) is calculated by predicting the required R-values for each of the plastics in the Scott phantom, which are set by initial calibration and standardisation at WAMMCO as 112% fat for polyethylene, 88% fat for Nylon, and 69% for Acrylic. This back-calculation is done by solving for Equation 9 with known *STLE* and *FatLean%*. These R-value predictions are plotted against the R-values of the plastics at the calibrated WAMMCO DXA, with the slope and intercept calculated

This project is supported by funding from the Australian Government Department of Agriculture, Fisheries and Forestry as part of its Rural R&D for Profit programme in partnership with Research & Development Corporations, Commercial Companies, State Departments & Universities.

and used to perform a linear transform on all *STR* values. A visualisation of this graph is seen in Figure 4:

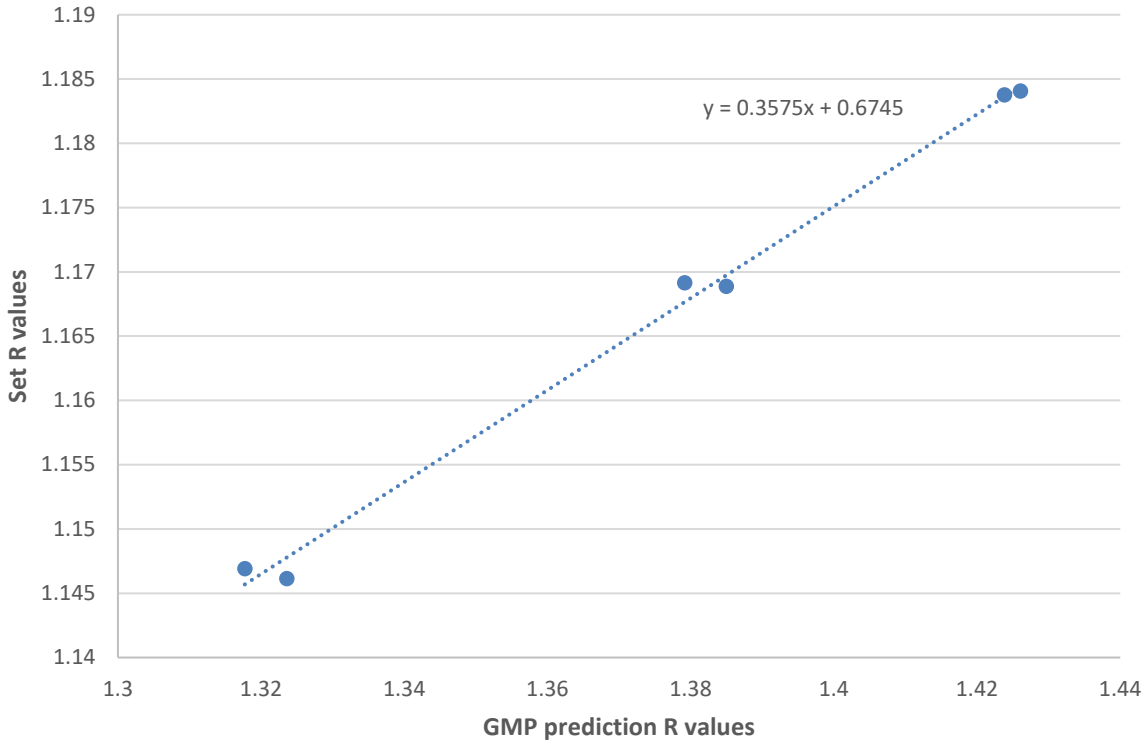

Figure 4 - Comparison of R-values from WAMMCO set phantom R-values for acrylic, polyethylene and nylon, against the GMP required R-values to produce the same FatLean% for each plastic type

The slope and intercept are used to adjust *STR*, which is used in the *FatLean%* calculation.

2.8 Final calculation

The final calculations performed are multiplying the *FatLean%* by the predicted soft tissue weight, which itself is divided by the total HCWT to produce the fat % and lean % predictions, as per:

$$Fat\ \% = \frac{\frac{FatLean\%}{100} * STWt}{HCWT} * 100 \qquad Eq.12$$

Similarly, the lean % is calculated in a similar way, by:

$$Lean\ \% = \frac{\frac{(100 - FatLean\%)}{100} * STWt}{HCWT} * 100 \qquad Eq.13$$

These are finalised with the bone % prediction to complete the predictions of CT composition.

2.9 HCWT prediction

This project is supported by funding from the Australian Government Department of Agriculture, Fisheries and Forestry as part of its Rural R&D for Profit programme in partnership with Research & Development Corporations, Commercial Companies, State Departments & Universities.

If HCWT is required to be predicted by the DXA image, a regressed model has been created by training 200 DXA images on known HCWT values, to produce the equation:

$$HCWT = 913.6148221 - 125.762918t - 704.2156856R + 0.0000295STA \\ -4.6424207BLE + 0.0000608BA + 99.8417547Rt \qquad Eq.14$$

Where *STA* is the area of soft tissue (in pixels), *BLE* is the thickness proxy for bone containing pixels, *BA* is the area of bone containing pixels. This produces highly precise and accurate predictions of HCWT to use in the full calculations mentioned above (see Figure 5), however is suggested to only be used if a HCWT is not available.

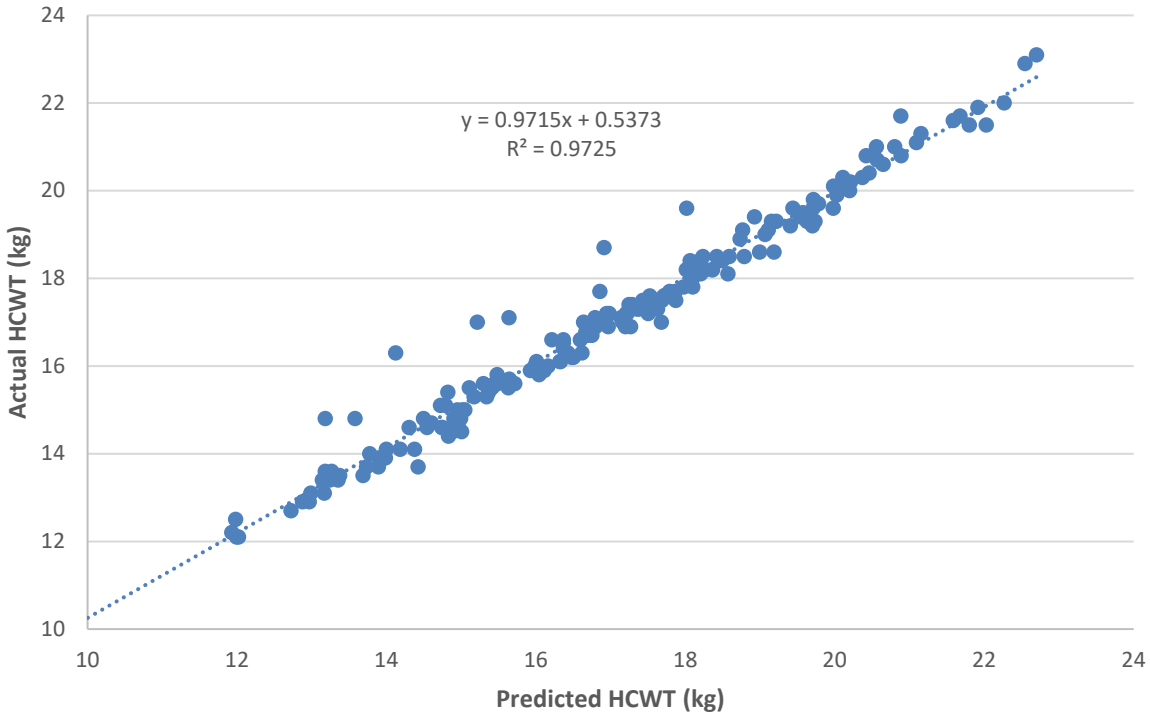

Figure 5 - DXA predicted HCWT vs Actual HCWT of 191 lambs

3 New vs Old Algorithm

3.1 Bone prediction

Prior to the introduction of the new bone detection and prediction component of this accredited algorithm, predictions of each component were good, except for bone %. There were modest increases in precision and accuracy, but the largest gain was in the prediction of bone % (see Table 1).

This project is supported by funding from the Australian Government Department of Agriculture, Fisheries and Forestry as part of its Rural R&D for Profit programme in partnership with Research & Development Corporations, Commercial Companies, State Departments & Universities.

Table 1 - R2, RMSE, Slope and Bias of the DXA predictions of CT fat %, lean % and bone % using the previous and accredited bone detection algorithms

	R^2	RMSE	Slope	Bias
Previous Algorithm				
Fat %	0.896	1.43%	0.97	-4.37
Lean %	0.809	1.36%	0.87	1.4
Bone %	0.925	0.61%	1.25	2.98
Accredited Algorithm				
Fat %	0.938	1.10%	0.97	-1.19
Lean %	0.716	1.66%	0.95	-0.23
Bone %	0.496	1.57%	1.05	1.41

See technical report for KPI 3.11 - Lamb DXA accreditation submission to AMILSC on behalf of Scott Automation and Robotics and MLA - for full visualisations of fat %, lean % and bone % gains in precision and accuracy.

3.2 Daily phantom adjustment

Small changes in accuracy are observed over multiple kill days at a single site, which therefore required small automated adjustments to the equation coefficients in the accredited algorithm to include for the calibration with the Scott phantom.

Below is a comparison of 400 lambs and their DXA prediction of fat % compared to CT fat % before (Figure 6) and after (Figure 7) adjustment of coefficients by the Scott phantom.

This project is supported by funding from the Australian Government Department of Agriculture, Fisheries and Forestry as part of its Rural R&D for Profit programme in partnership with Research & Development Corporations, Commercial Companies, State Departments & Universities.

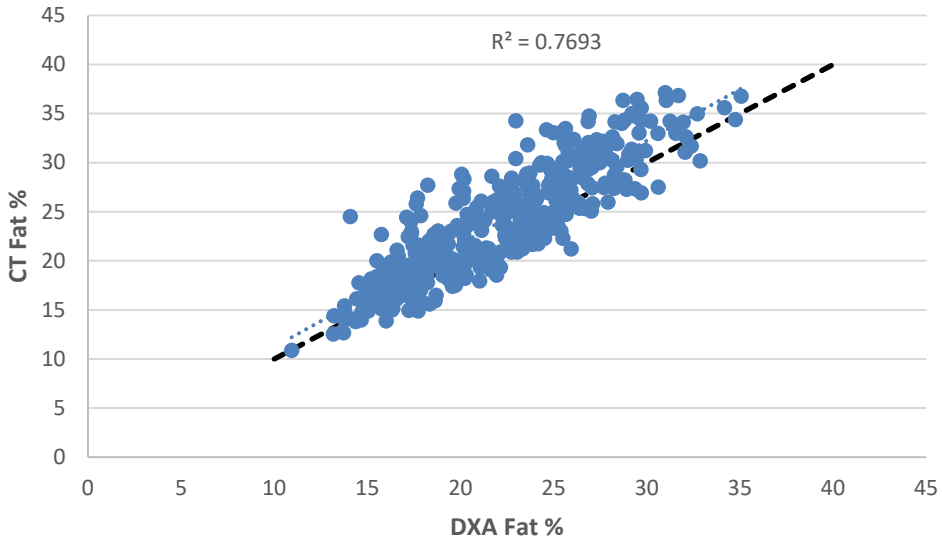

Figure 6 - DXA Predictions of fat % compared to CT fat % prior to any adjustments by phantoms. Dashed line represents line of perfect prediction.

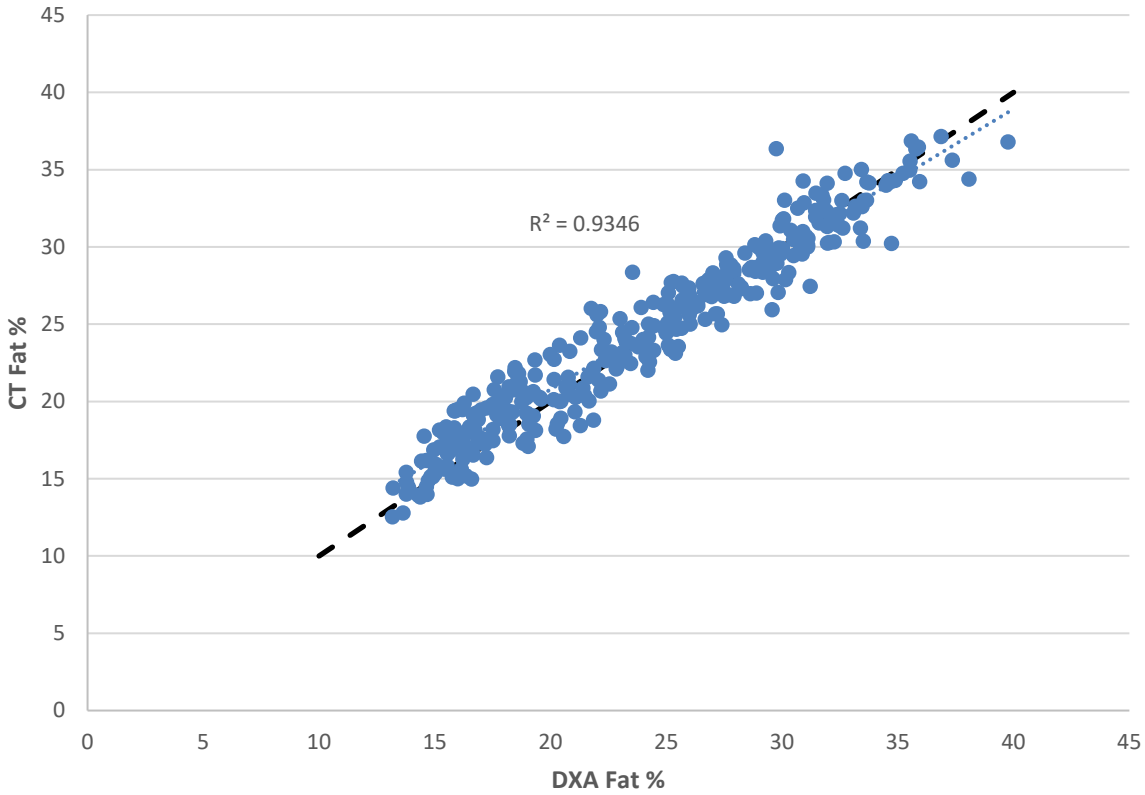

Figure 7 - DXA Predictions of fat % compared to CT fat % after adjustments by phantoms. Dashed line represents line of perfect prediction.

4 Future Work

This project is supported by funding from the Australian Government Department of Agriculture, Fisheries and Forestry as part of its Rural R&D for Profit programme in partnership with Research & Development Corporations, Commercial Companies, State Departments & Universities.

While each aspect of the accredited algorithm can be improved upon, however the limiting conditions as to the effectiveness of such improvements are a) the high level of precision of fat and lean predictions would mean that further improvements would be small and b) the computational power required for such fast calculations. Nevertheless, there are methods that can be implemented with further experimental work to improve upon the precision and accuracy of DXA predictions.

For bone detection and calculation, machine learning can be implemented to help detect bone edges. The identification of bone edges will allow for the entire region of bone to be correctly classified as such, and the bone containing pixels can also be evaluated more thoroughly for their bone content. The soft tissue within a bone-containing pixel can be isolated, and the bone mineral content can be calculated, furthering the data available for analysis. This process would increase computational time, however with the correct machine learning algorithm, this increase may still be within the required time (11-12 per minute).

The soft tissue component of the accredited algorithm would benefit from a more complex calibration technique, which would allow for the generation of the coefficients each day, rather than the adjustment of the coefficients. The use of plastic phantoms is logical, due to the ease of construction and reliability, however without a comparison to tissue values they are somewhat limited. A further calibration experiment using stearic acid and water would be a useful tool to create the correct coefficients for the prediction curve, with the appropriate plastics alongside as a comparison.

The use of such a phantom of tissue analogues would also serve as a useful tool for testing the accuracy and precision of a DXA unit for validating and accrediting existing and future devices.

This project is supported by funding from the Australian Government Department of Agriculture, Fisheries and Forestry as part of its Rural R&D for Profit programme in partnership with Research & Development Corporations, Commercial Companies, State Departments & Universities.

This project is supported by funding from the Australian Government Department of Agriculture, Fisheries and Forestry as part of its Rural R&D for Profit programme in partnership with Research & Development Corporations, Commercial Companies, State Departments & Universities.